Band structures of carbon nanotubes: the sp^{3}s* tight-binding model

LETTER TO THE EDITOR

Band structures of carbon nanotubes: the sp³s* tight-binding model

J X Cao[1,2]**, X H Yan**[1,3]**, J W Ding**[1,2] **and D L Wang**[1]

[1] Institute of Modern Physics and Department of Physics, Xiangtan University, Hunan, 411105, China
[2] Institute of Mechanics and Material Engineering, Xiangtan University, Hunan, 411105, China
[3] Institute of Solid State Physics, Chinese Academy of Sciences, Anhui, 230031, China

E-mail: caojuexian@263.net (J X Cao)

Abstract
We present a simple sp³s* tight-binding model for use in calculating the band structures of single-walled carbon nanotubes. The 2s, $2p_x$, $2p_y$, $2p_z$, and s* orbitals of each carbon atom are used as the basis set for expressing the tight-binding model, and the interatom interaction between neighbouring sites is fully taken into account. The elements of the Hamiltonian matrix and related parameters are obtained by adjusting the model to fit the primary reflectivity and photoemission band-structure data. We have employed this tight-binding model in investigating $[n, 0]$ ($n = 6, 7, 8, 9$) carbon nanotubes. Our band-structure and band-gap results show that [6, 0] and [9, 0] tubes are narrow-gap semiconductors rather than metallic ones, which is at variance with the findings of previous work.

The discovery of carbon nanotubes (CNTs) by Iijima [1] gave rise to intensive research on quasi-one-dimensional structures. As one of the most promising building blocks for the future development of functional nanostructures, CNTs can be used as 1D quantum wires, optical switches, nanotransistors, and other important electronic components. The individual single-walled CNTs have been predicted to be metallic or semiconducting on the basis of their diameters and chiralities [5–9]. Both of these factors determine the symmetry operations that describe the structure of CNTs, and consequently determine their electronic properties. Some efforts, both experimental and in theoretical calculations [9–12], have suggested that rehybridization of graphitic σ- and π-states should occur because of the curvature of the tubes. In 1999, Chen *et al* [13] displayed ultraviolet photoemission spectroscopy (UPS) He II spectra of CNTs and graphite, which provided evidence of the hybridization effect resulting from the formation of CNTs. To explain such an effect, many models, e.g. the graphite model and the sp³ tight-binding model, have been employed for single-walled CNTs. However, the graphite model and the classic sp³ model are too oversimplified to produce the conduction band and the indirect gaps because in each case some essential physical effect, e.g., the excited atomic states coupling with the anti-bonding p-like conduction states, is beyond the scope of

the consideration [16]. Considering the hybridization effect due to the effects of curvature in CNTs, we present a sp^3s^* tight-binding model for their band structure. Our model will successfully reproduce not only the valence bands but also the lowest conduction band, even permitting the treatment of CNTs with defects.

A single-walled CNT can be constructed conceptually by rolling up a single sheet of graphite along one of its two-dimensional lattice vectors $\vec{B} = n\vec{R}_1 + m\vec{R}_2$ to form a nanotube with diameter $D = a\sqrt{3(n^2 + nm + m^2)}/\pi$ and chiral angle $\theta = \arctan(\sqrt{3}m/[2n + m])$ [14,15] where a is the carbon–carbon-atom distance in a graphite sheet. Hence, it is convenient for us to specify general CNTs in terms of a pair of integers $[n, m]$. When $m = 0$, for example, a type of CNT classified as zigzag tubes is formed, whose diameter $D = \sqrt{3}na/\pi$ and chiral angle $\theta = 0°$, and an armchair tube with diameter $D = 3na/\pi$ and chiral angle $\theta = 30°$ can be obtained by taking $n = m$. An example of a [3, 2] nanotube is shown in figure 1. The vector $\vec{T}$ is the 1D translation vector of the nanotube along the axis. The unit cell marked as the rectangle in the figure involves $4(n^2 + nm + m^2)/d$ atoms with d the highest divisor of $(2n + m, 2m + n)$. Some related parameters for a $[n, m]$ nanotube are given in table 1. The carbon-atom hexagons on each tube are arranged in a helical fashion about the tube axis.
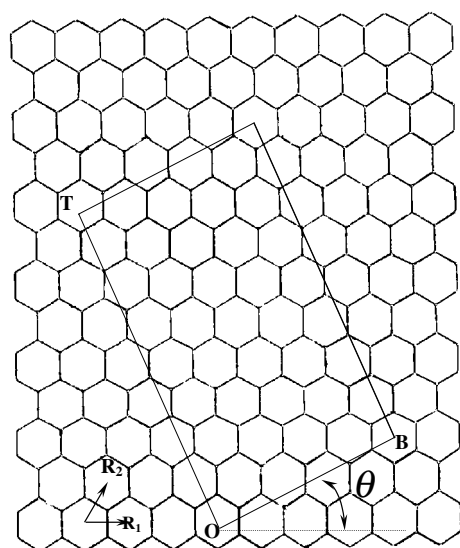

Figure 1. Depiction of a graphite sheet for the [3, 2] nanotube.

Table 1. Some parameters for $[n, m]$ carbon nanotubes.

Symbol	Name	Formula
a	Carbon–carbon distance in graphite sheet	1.421 Å
$\vec{R}_1, \vec{R}_2$	Unit vector	$(1, 0), (1/2, \sqrt{3}/2)$
$\vec{B}$	Chiral vector	$\vec{B} = n\vec{R}_1 + m\vec{R}_2$
L	Circumference of nanotube	$L = a\sqrt{3(n^2 + nm + m^2)}$
d	Highest common divisor of $(2n + m, 2m + n)$	
$\vec{T}$	Translation vector of the 1D unit cell	$\vec{T} = t_1\vec{R}_1 + t_2\vec{R}_2$
$|\vec{T}|$	Length of $\vec{T}$	$|\vec{T}| = \sqrt{3}L/d$
N	Number of atoms per unit cell	$N = 4(n^2 + nm + m^2)/d$
θ	Chiral angle	$\theta = \arctan(\sqrt{3}m/[2n + m])$

The proper boundary conditions around the tube can only be satisfied if one of the Bravais lattice vectors of the graphite sheet maps to a circumference around the tube [15]—that is, $\vec{K} \cdot \vec{B} = 2\pi m$ with m being an integer and $\vec{K}$ an allowed state of the CNT. We performed a band-structure calculation for $[n, 0]$ ($n = 6, 7, 8, 9$) tubes by using the sp^3s^* tight-binding model. The 2s, $2p_x$, $2p_y$, $2p_z$, and the excited-s-state s* orbitals of each atom are used as the basis set for expressing the tight-binding model, and the nonorthogonality of the atomic orbital between neighbouring sites is fully taken into account.

The sp^3s^* model was recommended by Vogl and co-workers for use in band-structure calculations for zinc-blende-structure semiconductors [16]. In the present letter, we have developed this model and applied it to CNTs. The Bloch functions used in our model can be described as follows:

$$|\Psi_\lambda(\vec{k}, \vec{r})\rangle = \frac{1}{\sqrt{N}} \sum_m e^{i\vec{k}\cdot\vec{R}_m} |\varphi_\lambda(\vec{r} - \vec{R}_m - \vec{\tau}_M)\rangle$$

where the number λ runs over the s, p_x, p_y, p_z, and s* orbitals and $\vec{\tau}_M$ is the relative displacement of the Mth atom in the unit cell. The wave vector $\vec{k}$ lies in the first Brillouin zone. $\vec{R}_m$ is the translation vector along the axis of the nanotube. The Hamiltonian matrix in terms of the basis set $|\varphi_\lambda(\vec{r} - \vec{R}_m - \vec{\tau}_M)\rangle$ is detailed in table 2, where it is assumed that the jth atom is a nearest atom to the ith atom and the lth atom is not.

Table 2. The elements of the Hamiltonian matrix.

	ith atom	jth atom	lth atom
ith atom	$\mathbf{E}_1$	$\sum_m e^{i\vec{k}\cdot\vec{d}_{ij}} \mathbf{E}(\vec{d}_{ij})$	$\mathbf{E}_0$
jth atom	$\sum_m e^{i\vec{k}\cdot\vec{d}_{ji}} \mathbf{E}(\vec{d}_{ji})$	$\mathbf{E}_1$	
lth atom	$\mathbf{E}_0$		$\mathbf{E}_1$

In table 2, $\mathbf{E}_1$, $\mathbf{E}_0$, and $\mathbf{E}(\vec{d}_{ij})$ are 5×5 matrices. The five diagonal matrix elements of $\mathbf{E}_1$ are determined by the s-, p-, and s*-orbital energies of each atom and the rest are zero. All of the elements of the matrix $\mathbf{E}_0$ will vanish because we just take the nearest-neighbour interaction into account. Following Slater–Koster tables, we assumed the elements of $\mathbf{E}(\vec{d}_{ij})$ to be as in table 3, where l, m, n are the direction cosines of $\vec{d}_{ij} = \vec{\tau}_i - \vec{\tau}_j$ with respect to x, y, and z, respectively. Our model parameters are given by $V_{ss\sigma} = 4.76$ eV, $V_{sp\sigma} = 4.33$ eV, $V_{pp\pi} = -2.77$ eV, $V_{pp\sigma} = 4.37$ eV [13]. The other two parameters, $V_{s^*p\sigma}$, $V_{s^*s^*\sigma}$, can be obtained from table 1 in reference [16]. We have adjusted our tight-binding model to fit the primary reflectivity and photoemission band-structure data.

Table 3. The elements of the Hamiltonian matrix $\mathbf{E}(\vec{d}_{ij})$.

	s	p_x	p_y	p_z	s*
s	$V_{ss\sigma}$	$l V_{sp\sigma}$	$m V_{sp\sigma}$	$n V_{sp\sigma}$	0
p_x	$l V_{sp\sigma}$	$l^2 V_{pp\sigma} + (1 - l^2) V_{pp\pi}$	$lm(V_{pp\sigma} - V_{pp\pi})$	$ln(V_{pp\sigma} - V_{pp\pi})$	$l V_{s^*p\sigma}$
p_y	$m V_{sp\sigma}$	$lm(V_{pp\sigma} - V_{pp\pi})$	$m^2 V_{pp\sigma} + (1 - m^2) V_{pp\pi}$	$nm(V_{pp\sigma} - V_{pp\pi})$	$m V_{s^*p\sigma}$
p_z	$n V_{sp\sigma}$	$ln(V_{pp\sigma} - V_{pp\pi})$	$nm(V_{pp\sigma} - V_{pp\pi})$	$n^2 V_{pp\sigma} + (1 - n^2) V_{pp\pi}$	$n V_{s^*p\sigma}$
s*	0	$l V_{s^*p\sigma}$	$m V_{s^*p\sigma}$	$n V_{s^*p\sigma}$	$V_{s^*s^*\sigma}$

We have used our model to investigate $[n, 0]$ (n runs from 6 to 9) CNTs, and their band structures are shown in figure 2 and the band gaps are given in table 4, where the results obtained by Blase *et al* [12] are also given for comparison. The band structures in figures 2(b) and 2(c)
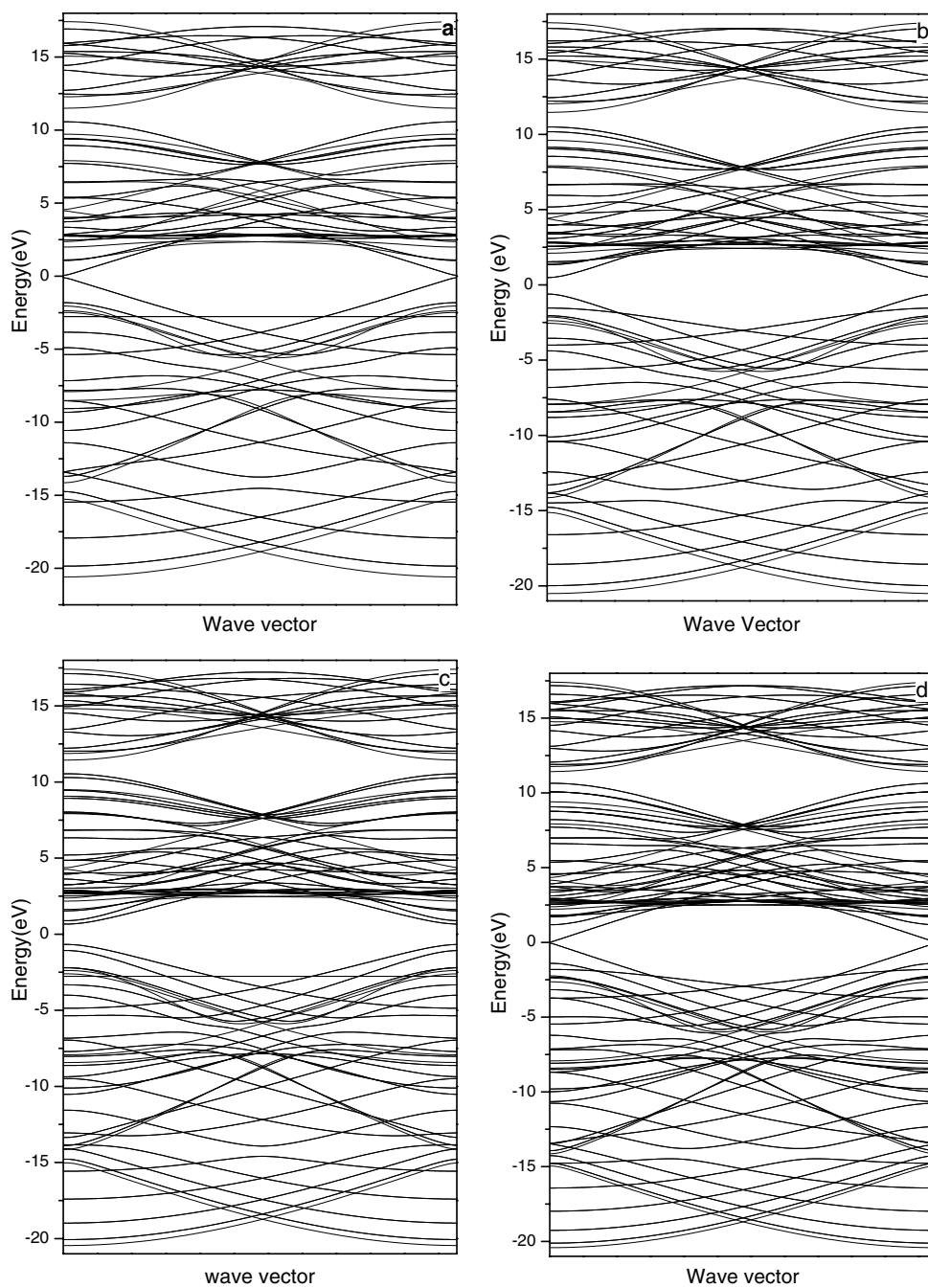
Figure 2. The band structures of the (a) [6, 0], (b) [7, 0], (c) [8, 0], and (d) [9, 0] carbon nanotubes.

show that [7, 0] and [8, 0] tubes are semiconductors with gaps of about 1 eV, which is consistent with the results given by Blase *et al* on the basis of an sp^3 TB model, while the energy gaps are much larger than those obtained with the local density approximation (LDA). In addition, Blase *et al* have shown that the [6, 0] tube is metallic while the [9, 0] tube is a narrow-gap

Table 4. The band gaps of the [n, 0] tubes.

| Tube | Our sp^{3}s* TB model | | | The sp^3 TB model [12] | The LDA [12] |
	Bottom of the conduction band (eV)	Top of the valence band (eV)	Energy gap (eV)	Energy gap (eV)	Energy gap (eV)
[6, 0]	0.0558	−0.1133	0.1791	0.05	−0.83
[7, 0]	0.4656	−0.5808	1.0463	1.04	0.09
[8, 0]	0.5643	−0.5723	1.1866	1.19	0.62
[9, 0]	0.0249	−0.0505	0.0754	0.07	0.17

semiconductor. However, with our sp^{3}s* TB model, we found that [6, 0] and [9, 0] tubes each have a gap opening, at about 50 meV and 70 meV (see table 4), respectively. It is shown that they are narrow-gap semiconductors rather than metallic, while they are predicted to be metallic by previous work [17, 18]. Such a difference may be caused by the excited s* states coupling with the anti-bonding p-like conduction states while the graphite sheet is being rolled into a nanotube.

References

[1] Iijima S 1991 *Nature* **354** 56
[2] Tans S J *et al* 1997 *Nature* **386** 474
[3] Bockrath M *et al* 1997 *Science* **275** 1922
[4] Collins P G, Zettl A, Bando H, Thess A and Smalley R E 1997 *Science* **278** 100
[5] Robertson D H, Brenner P W and Mintmire J W 1992 *Phys. Rev.* B **45** 12 592
[6] Jishi R A, Bargin J and Lou L 1999 *Phys. Rev.* B **59** 9862
[7] Jishi R A *et al* 1994 *J. Phys. Soc. Japan* **63** 252
[8] White C T, Robertson D H and Mintmire J W 1993 *Phys. Rev.* B **47** 5485
[9] Hamada N, Sawada S and Oshiyama A 1992 *Phys. Rev. Lett.* **68** 1579
[10] Saito R, Fujita M, Dresselhaus G and Dresselhaus M S 1992 *Appl. Phys. Lett.* **60** 2204
[11] Mintmire J W, Dunlap B I and White C T 1992 *Phys. Rev. Lett.* **68** 631
[12] Blase X, Benedict L, Shirley E L and Louie S G 1994 *Phys. Rev. Lett.* **72** 1878
[13] Chen P, Wu X, Sun X, Lin J, Ji W and Tan K L 1999 *Phys. Rev. Lett.* **82** 91 578
[14] Mintmire J W and White C T 1995 *Carbon* **33** 893
[15] Dresselhaus M S, Dresselhaus G and Saito R 1995 *Carbon* **33** 883
[16] Vogl P, Hjalmarsson H P and Dow J D 1983 *J. Phys. Chem. Solids* **44** 365
[17] White C T and Mintmire J W 1998 *Nature* **394** 29
[18] Dresselhaus M S 1998 *Nature* **391** 19